submicro-metric SiO-2 spheres," Appl. Phys. Lett. **71,** 1148 (1997).
6. O. Kalinina, E. Kumacheva, "A core-shell approach to producing 3D polymer nanocomponents," Macromolecules **32,** 4122 (1999).

CTuB2 **2:45 pm**

Optical properties of ordered macroporous materials made by colloidal assembly

J.D. Thorne, D.J. Pine, G. Subramanian,*
Chemical Engineering Department, University of California, Santa Barbara, USA; E-mail: thorne@engineering.ucsb.edu

There is currently a major interest in the design and fabrication of periodic dielectric structures exhibiting photonic bandgaps (PBG)[1] at optical and near-infrared frequencies. Apart from their applications in catalysis and separations processes, PBG materials also have several unique optical properties, such as inhibition of spontaneous emission or photon localization.[2,3]

Calculations show that a variety of periodic dielectric structures exhibit PBGs. An important requirement for achieving observable bandgaps is that the materials be constructed from materials with high dielectric contrast. The range of wavelengths of the PBG is determined by the periodicity of the voids. Thus, to achieve a PBG in the visible, lattice spacings should scale with the wavelength of visible light. A promising approach to making PBG's at optical frequencies is to use colloids as self-assembled templates. Monodisperse colloids self-assemble into three-dimensional crystals with excellent long-range order at optical length scales. The ordered arrays can then act as a scaffold around which a high dielectric material can be synthesized.

We have used this idea to make periodic macroporous materials using a simple and effective method.[4] Our technique employs monodisperse polystyrene as templates and ultrafine (<100 nm) metal oxide particles as the surrounding high dielectric material. The process involves slowly drying a monodisperse polystyrene dispersion with a colloidal dispersion of the desired oxide. As the mixture is drying, the polystyrene spheres organize themselves in an ordered lattice and the oxide particles pack into the voids between the spheres. Subsequent removal of the polystyrene by heat treatment leads to an ordered macroporous material with the oxide particles forming the walls of the pores. We have made macroporous silicon dioxide and titanium dioxide with this method. Figure 1 shows a scanning electron microscope (SEM) micrograph of macroporous titanium dioxide.

Optically, these materials exhibit a strong iridescence in reflected light. Optical reflectivity measurements were measured to probe the existence of band gaps in the material. The reflectivity spectra of macroporous titanium dioxide is shown in Fig. 2. The peaks in reflectivity correspond to Bragg reflections from the ordered porous structure, The full width at half maximum of these peaks lie between 12 and 14% and is related to the strength of the interaction between light and the ordered structure.

Chemical Engineering Department and Materials Res. Lab., Univ. of California, Santa Barbara, USA

1. J.D. Joannopoulos, R.D. Meade, J.N. Winn, *Photonic crystals: molding the flow of light* (Princeton Univ. Press, Princeton, N.J., 1995).
2. E. Yablonovitch, "Inhibited spontaneous emission in solid-state physics and electronics," Phys. Rev. Lett. **58,** 2059–2062 (1987).
3. S. John, "Strong localization of photons in certain disordered dielectric superlattices," Phys. Rev. Lett. **58,** 2486–2489 (1987).
4. G. Subramanian, V.N. Manoharan, J.D. Thorne, D.J. Pine, "Ordered macroporous materials by colloidal assembly: a possible route to photonic band gap materials," Adv. Mater. **11,** 1261–1265 (1999).

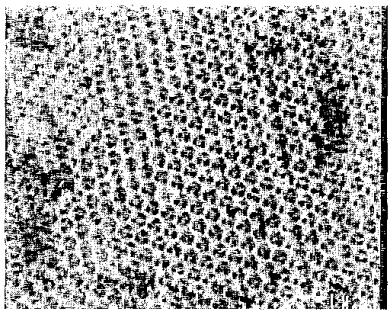

CTuB2 Fig. 1. SEM micrograph of an interior surface of macroporous titania made with 550-nm polystyrene spheres.

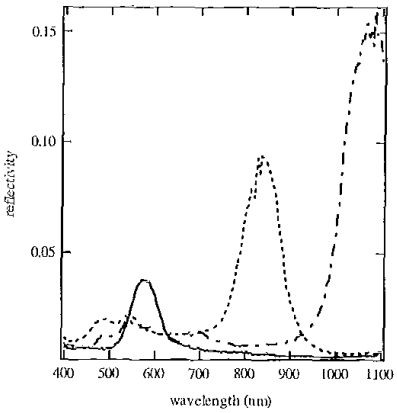

CTuB2 Fig. 2. Optical reflecitivity spectra of macroporous titanium dioxide. Peaks centered at 570, 840, and 1080 nm correspond to air holes of 320, 440, and 525 nm in diameter respectively. The reflected light was detected at an angle of 35 ± 2 degrees with respect to the incident beam.

CTuB3 **3:00 pm**

Highly doped silicon micromachined photonic crystals

B. Temelkuran, Mehmet Bayindir, E. Ozbay, J.P. Kavanaugh,* M.M. Sigalas,* G. Tuttle,*
Department of Physics, Bilkent Univ., Bilkent, 06533 Ankara, Turkey; E-mail: burak@fen.bilkent.edu.tr

Photonic crystals are periodic structures with the property of reflecting the electromagnetic (EM) waves in all directions within a certain frequency range. These structures can be used to control and manipulate the behaviour of EM waves. Although earlier work concentrated on building these crystals with dielectric materials, there are certain advantages of introducing metals to photonic crystals.[1] First, metals offer a high rejection rate when compared to the dielectric crystals. Second, for microwave applications, the dimensions of metallic crystals can be kept much smaller than the minimum dimensions needed for a typical dielectric crystal. In this paper, we will propose a method for the fabrication of layer-by-layer metallic photonic crystals. A similar method had been used by Ozbay *et al.* to fabricate dielectric photonic crystals using silicon wafers.[2]

We fabricated a new layer-by-layer photonic crystal using highly doped silicon wafers. Because resistivity of a silicon wafer decreases with the doping concentration, we predicted that due to the low resistivity of layers, this structure will show metallic photonic crystal properties, exhibiting a metallicity gap with an upper band edge around 100 GHz, with the new dimensions. We use the anisotropic etching of silicon by aqueous potassium hydroxide (KOH), which etches the 100 planes, and the planes making 45° to the 110 planes of silicon at equal rates, and resulting in flat walls at the etched perpendicular surfaces.[3]

The (100) silicon wafers used in this work were each 3 in. in diameter and 400-μm thick. The resistivity of wafers were in the range 0.0015–0.004 Ωcm. In the first step of the process, one side of the wafers are coated with a nitrate film of thickness 1 μm, at 250°C using

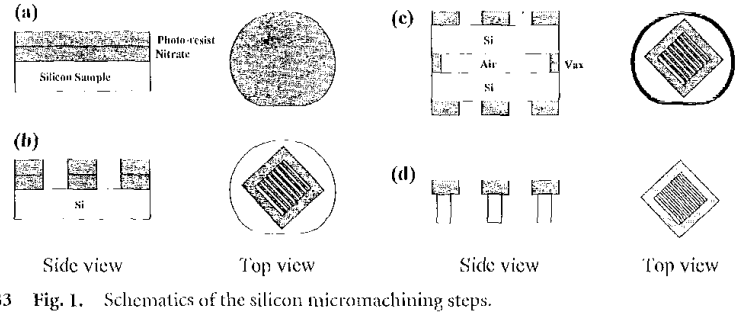

CTuB3 Fig. 1. Schematics of the silicon micromachining steps.

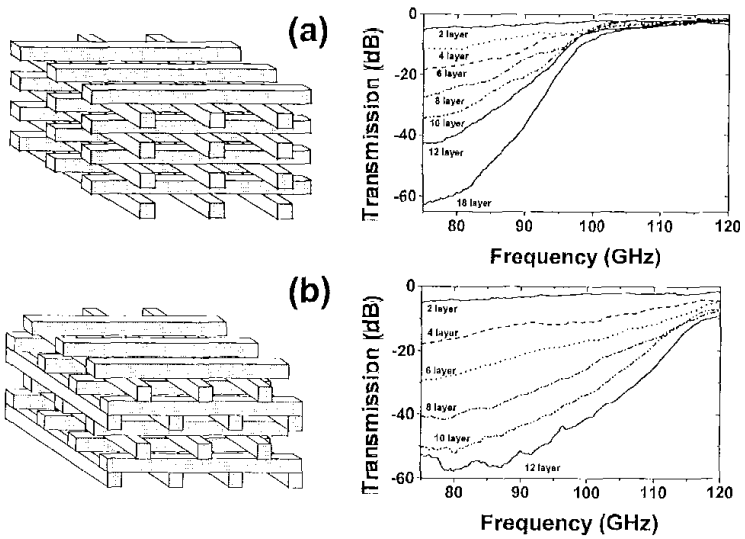

CTuB3 Fig. 2. Schematics (left panel) and the transmission characteristics (right panel) of (a) st and (b) fct layer-by-layer photonic crystals.

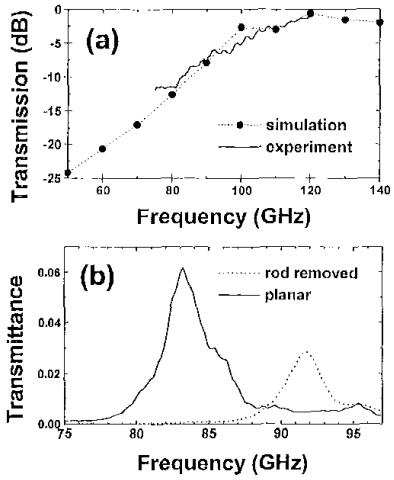

CTuB3 Fig. 3. (a) Measured (solid line) and simulated (dotted line) transmission characteristics of a four layer st type crystal structure. (b) Transmission characteristics of planar defect (solid line) and single rod removed defect (dotted line) built around fct type photonic crystal.

plasma enhanced chemical vapour deposition (PECVD). Nitrate film must serve as a mask during the anisotropic etching step, and we found out that this thickness and growth temperature was suitable for this purpose. Next, the nitrate was patterned by conventional photolithography and aqueous hydrofloric acid (HF) etching [Fig. 1(a)]. The pattern consists of 19 parallel stripes, each 960-μm wide and with center-to-center separation of 1600 μm. These stripe dimensions and the wafer thickness determine the upper band-edge, calculated to be around 100 GHz. The stripes are at an angle of 45° to the 110 plane of the silicon, as defined by the major flat of the wafer. A 1.5-cm-wide border around the stripe-array is protected by the photoresist, with the outer regions of the wafer left exposed so that a square will be left after etching. Within the border region are four small rectangular openings that will serve as guide holes for the stacking process. After the nitrate layer is patterned [Fig. 1(b)], in order to protect back sides of the wafers, we cover the most outer parts of each samples back side, and stick it to a smooth surface which was not etched by KOH solution. In order to save space and time, we prefer to stick it back-to-back with another ready-to-etch sample [Fig. 1(c)]. The wafers are then dipped into an aqueous KOH solution. A typical etch performed in a 25% KOH solution at a temperature of 55°C (below the melting temperature of vax) takes about 24 hours to etch entirely through the wafer. Due to the etching profile of silicon with KOH, the rods are also etched ~400 μm from both sides, which is thickness of the wafer. So, rods become approximately $960 - (2 \times 400) = 160$ μm wide at the end of the etching. All layers are further etched the necessary time to equalize rod thicknesses to 150 μm. Finally, the vax is removed by trichloroethane (TCA), and the remaining nitrate is removed by HF, and the wafers are stacked to form photonic crystal using a holder having pins that align to the guide holes.

Once fabrication was completed, transmission properties of the crystal were measured with a W-band (75–120 GHz) measurement arrangement. A Ku-band frequency synthesizer was used to generate the signal that was first amplified and then multiplied in frequency by six times to reach the W band. The high frequency signal was radiated by a standard-gain horn antenna (aperture size of 1.17 cm × 1.45 cm), and the transmitted radiation was collected by a second horn antenna. The amplitude of the received signal was measured using a harmonic mixer and a network analyzer.

As shown in Fig. 2 (left panel), the wafers may be stacked to form simple tetragonal (st) or face centered tetragonal (fct) type of crystals.[1] The transmission spectra of each crystal as the number of layers are increased are exhibited on right panel. The upper edge of the bandgap for st crystal is located at 105 GHz, and for fct crystal around 120 GHz. No lower band edge is detected within the measurable frequency range, consistent with the theory that predicted a bandgap extending down to zero frequencies. This metallicity gap verifies the prediction that our crystals are analogous to metallic photonic crystals.[1] Around 80 GHz, the attenuation per layer is around 3.5–4 dB for st structure, and is 5.5–6 dB for fct structure. Within the metallicity gap of both of the crystals, we observe full reflection of the EM wave. Figure 3(a) shows the transmission from 4 layer st type of crystal (solid line), which agrees well with the transfer matrix method simulation results (dotted line).

It was previously shown in other metallic layer-by-layer photonic crystals that defect structures around this geometry can be built by means of adding or removing rods from an otherwise perfect crystal.[4] The same idea was used to investigate the defect characteristics of these semiconductor based photonic crystals. The defect modes for this structure show Q factors around 30. Figure 3(b) (dotted line) shows the transmission through a 9 layer fct type of crystal, with a single rod missing from the 5th layer of the crystal. The resonance frequency of the defect mode is at 91.8 GHz, with a Q factor of 30.

We then investigated a planar type of defect structures, built around an 8 layer st based photonic crystal. The planar defect was obtained by separating the 4th and 5th layers of the crystal. This resulted in a planar air gap between the two photonic mirrors, each formed of a 4 layer (2 unit cell) crystal. These planar defects also resulted in similar defect characteristics, however with higher transmission amplitudes. Figure 3(b) (solid line) shows transmission through the planar defect of separation width $L = 650$ μm. The defect frequency, which is 83.2 GHz for this case, can be tuned within the band gap by changing the width of the cavity as we have investigated in the previous dielectric and metallic photonic crystal structures.[1]

In conclusion, using standard semiconductor micromachining techniques, we fabricated a new layer-by-layer photonic crystals. These crystals exhibited a metallicity gap with an upper band edge around 100 GHz. The rejection rate per layer obtained from fct type of crystals (5.5–6 dB) were found to be superior to rejection rates of similar dielectric photonic crystal structures (3.5–4 dB per layer). Localization of the EM field is possible with defects created around these structures by removing rods or introducing planar cavities. By using special silicon thinning methods and double etching the wafers on both surfaces, the frequency range of this fabrication technology could probably be extended to built structures with photonic bandgaps as high as 10 THz.

*Iowa State Univ., USA

1. B. Temelkuran, H. Altug, E. Ozbay, "Experimental investigation of layer-by-layer metallic photonic crystals," IEE Proc.-Optoelectron. **145**, 409–414 (1998).
2. E. Ozbay, E. Michel, G. Tuttle, R. Biswas, M.M. Sigalas, K.M. Ho, "Micromachined millimeter-wave photonic bandgap crys-

tals," Appl. Phys. Lett. **64,** 2059–2061 (1994).
3. E. Bassous, in Symposium on Electrochemical Thechnology in electronics, edited by L.T. Romankiw, T. Osaka, (Electrochemical Society, Pennington, NJ, 1987), p. 616.
4. E. Ozbay, B. Temelkuran, G. Tuttle, M. Sigalas, C.M. Soukoulis, K.M. Ho, "Defect structures in metallic photonic crystals," Appl. Phys. Lett. **69,** 3797–3799 (1996).

CTuB4 **3:15 pm**

Photo-thermo-refractive glasses for high-efficiency Bragg gratings in UV, visible, and IR regions

O.M. Efimov, H. Francois-Saint-Cyr, L.B. Glebov, L.N. Glebova, K. Richardson, V.I. Smirnov, *CREOL, Univ. of Central Florida, P.O. Box 162700, Orlando, Florida 32816-2700, USA; E-mail: leon@mail.creol.ucf.edu*

The wide spread use of holographic elements is constrained by the lack of available holographic materials. Hariharan's recent book[1] notes that among the photosensitive materials available for high efficiency hologram recording, each have merits, as well as drawbacks. This paper describes properties and performance of inorganic glass as a medium for volume hologram recording, which meets most requirements cited. The use of inorganic photosensitive glasses for phase hologram recording was described several years ago (see survey in Ref. [2]). The two-step process of exposure to UV radiation and thermal development (photo-thermo-refractive process) has been used to record phase patterns in glass defined as photo-thermo-refractive (PTR). Relative diffraction efficiency of up to 90% was recorded at that time, however, strong scattering from the thermal development process resulted in a low absolute diffraction efficiency, not exceeding 45%.

Recent efforts have successfully concentrated on the proper choice of glass processing technology and exposure and thermal development conditions, to eliminate undesirable scattering. The results of recent progress in photosensitive glass with approximate composition (mol. %) $15Na_2O$-$5ZnO$-$4Al_2O_3$-$70SiO_2$-$5NaF$-$0.01\ Ag_2O$-$0.01CeO_2$, have been summarized.[3] Glasses were exposed with 325-nm radiation and developed at 520°C to obtain gratings with spatial frequencies ranging from 250 mm^{-1} to 9200 mm^{-1}.

The photosensitivity of PTR glass ranges from 280 to 360 nm. Absorption of PTR glass was found to be less than 0.01 cm^{-1} in the visible and near IR regions and below 1 cm^{-1} in spectral ranges 280–380 nm and 2700–4200 nm. Thus, holograms in this glass can be successfully used for all lasers and optical communication wavelengths in the near UV, visible, and near IR regions (Fig. 1). For specimens exposed using doses of 50 mJ/cm^2 to 5 J/cm^2, the induced refractive index decreased monotonically to 10^{-3}, during the development process. No dependence of diffraction efficiency on spatial frequency was observed between 250 mm^{-1} to 3000 mm^{-1}. Moreover, relative diffraction efficiency in the UV region of ~50% was obtained for a spatial frequency of 9200 mm^{-1}. The diffraction efficiency of Bragg gratings in PTR glasses did not decrease upon heating to 400°C and no fading was observed with exposure to UV, visible and IR radiation. The laser-induced damage threshold in exposed and developed PTR glass was about 30% of that in standard optical glass BK-7.[4]

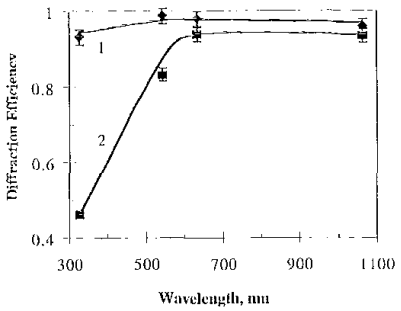

CTuB4 Fig. 1. Diffraction efficiency of transmitting Bragg gratings in PTR glass for different wavelengths in UV, visible and IR spectral regions. 1– relative and 2– absolute diffraction efficiency.

1. P. Hariharan. Optical Holography. Principles, techniques, and applications. Chapter 7: "Practical recording materials," 95–124. Cambridge Univ. Press, 1996. p. 95.
2. L.B. Glebov, "Photosensitive glass for phase hologram recording," Glastech. Ber. Glass Sci. Technol. **71C,** 85–90 (1998).
3. O.M. Efimov, L.B. Glebov, L.N. Glebova, K.A. Richardson, V.I. Smirnov, "High-Efficiency Bragg Gratings in Photothermorefractive Glass," Appl. Optics, Optical Technology and Biomedical Optics (OT&BO), **38,** 619–627 (1999).
4. O.M. Efimov, L.B. Glebov, S. Papernov, A.W. Schmid, "Laser-induced damage of photo-thermo-refractive glasses for optical-holographic-element writing," Proc. SPIE **3578,** 554–575 (1999).

CTuB5 **3:30 pm**

Polarization dependent surface photomodulation in As_2S_3 chalcogenide glass

Ali Saliminia, Tigran Galstian, Alain Villeneuve, Kathleen Richardson,* Amy Graham,* Cedric Lopez,* Sudipta Seal,* D.K. Verma,* Alfons Schulte,* *COPL, Department of Physics, Laval Univ., Québec, Canada, G1K 7P4; E-mail: asalimin@phy.ulaval.ca*

Over the past few years, high photosensitivity of chalcogenide glasses (ChG) has provided several applications in the field of optical communication.[1] Among photosensitive effects, photodarkening and photoexpansion have been extensively studied, and a variety of applications have emerged such as holographic microlenses, diffraction gratings, and Bragg reflectors.[2–4] The chemical and structural reasons for such changes are the subject of current investigations within our group.[5] Giant photo-

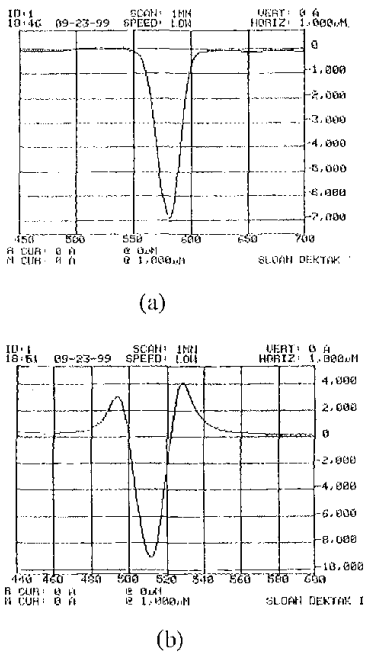

CTuB5 Fig. 1. (a) Surface profile probed perpendicular to the polarization direction, power ~10 mW, illumination size ~50 μm, exposition time ~480 sec, (b) Surface profile illustrated in (a), probed along the polarization direction.

expansion (2–5%) in As_2S_3 glass (E_g ~ 2.35 eV),[6] revealed surface expansions almost 10 times greater than that observed by conventional photoexpansion.

To date, no investigation has been carried out regarding the dependence of surface deformation on the polarization of light. In this work, we report, for the first time to our knowledge, the observation and study of a giant (~30–40%) polarization-dependent photoinduced surface deformation in As_2S_3 thin films.

A 2-μm-thick As_2S_3 thin film was prepared by the thermal evaporation (10^{-7} Torr, ~3 nm/sec) onto a transparent microscope slide. The focused single beam of an Ar^+ laser (514 nm) with Gaussian intensity profile was used to illuminate the sample. The sample was placed near the focal plane of a lens (f = 95 mm), and two half and quarter wave plates were used to expose the sample with linear or circular polarization. The small regions (~50 μm) were exposed under different powers of 5–80 mW during 30–600 sec. A profilemeter (DekTak) and AFM were used to measure the obtained surface deformations.

Surface profiles showing dip and pileup regions were measured. For excitation by a linear polarized light, it was found that the direction of pileup formation strongly depends on the direction of polarization. That is, as shown in Fig. 1, a dip and two pileups were detected along the polarization, while no pileup was observed for perpendicular direction to the polarization. The size of the deformed area was approximately equal to the beam width. Moreover, a symmetric pattern of uniformly formed pileups around the dip was detected for excitation by the circular polarized light, as illustrated in Fig. 2.